Springer Proceedings in Energy

Younes Chiba
Abdelhalim Tlemçani
Arezki Smaili *Editors*

Advances in Green Energies and Materials Technology

Selected Articles from the Algerian Symposium on Renewable Energy and Materials (ASREM-2020)

Springer

Springer Proceedings in Energy

The series Springer Proceedings in Energy covers a broad range of multidisciplinary subjects in those research fields closely related to present and future forms of energy as a resource for human societies. Typically based on material presented at conferences, workshops and similar scientific meetings, volumes published in this series will constitute comprehensive state-of-the-art references on energy-related science and technology studies. The subjects of these conferences will fall typically within these broad categories:

- Energy Efficiency
- Fossil Fuels
- Nuclear Energy
- Policy, Economics, Management & Transport
- Renewable and Green Energy
- Systems, Storage and Harvesting
- Materials for Energy

eBook Volumes in the Springer Proceedings in Energy will be available online in the world's most extensive eBook collection, as part of the Springer Energy eBook Collection. To submit a proposal or for further inquiries, please contact the Springer Editor in your region:

Kamiya Khatter (India)
Email: kamiya.khatter@springer.com
Loyola D'Silva (All other countries)
Email: loyola.dsilva@springer.com

More information about this series at http://www.springer.com/series/13370

Younes Chiba · Abdelhalim Tlemçani ·
Arezki Smaili
Editors

Advances in Green Energies and Materials Technology

Selected Articles from the Algerian Symposium on Renewable Energy and Materials (ASREM-2020)

Springer

Editors
Younes Chiba
Department of Mechanical Engineering
University Yahia Fares of Medea
Médéa, Algeria

Abdelhalim Tlemçani
Department of Electrical Engineering
University Yahia Fares of Medea
Médéa, Algeria

Arezki Smaili
Department of Mechanical Engineering
National Polytechnic School-ENP
Algiers, Algeria

ISSN 2352-2534 ISSN 2352-2542 (electronic)
Springer Proceedings in Energy
ISBN 978-981-16-0377-8 ISBN 978-981-16-0378-5 (eBook)
https://doi.org/10.1007/978-981-16-0378-5

Preface

This proceeding contains selected papers presented in the Algerian Symposium on Renewable Energy and Materials (ASREM-2020), which was held at University of Medea, Medea city, Algeria. The symposium aims to provide a platform for students, engineers, researchers and scientists to share their knowledge and ideas in the recent trends in the field of renewable energy and materials. Various aspects of clean energy are covered in this symposium, including (but not limited to) renewable energy systems, materials engineering, numerical modeling, hydrogen energy and conventional energy systems. The photothermal and photovoltaic can be considered the hot topic at the symposium. This is because Algeria has one of the most important solar energy resources in the world, and the recent government renewable energy and energy-saving development program. Over 250 submitted papers were received, and after a rigorous peer-reviewed process, 150 papers have been accepted, of which 100 for oral presentation and the remaining for a poster presentation.

We would like to take this opportunity to thank our sponsors (Medea University, Djelfa University, LAADI, ESLI, ENTEC, SINALE, CARSI, SONELGAZ, ATRST, DGRSDT) and Springer. Also, we offer our sincere thanks to the members of organizing and steering committees of the symposium, dean of technology faculty and rector of the university for their help, ongoing and enthusiastic support.

Médéa, Algeria — Younes Chiba
Médéa, Algeria — Abdelhalim Tlemçani
Algiers, Algeria — Arezki Smaili
October 2020

Contents

About the Editors

Younes Chiba is currently an associate professor on Mechanical Engineering Department, Faculty of Technology, University of Médéa, Algeria, since 2006. He specializes in Clean Energy and Materials. He received his M.Sc. in HVAC systems from Constantine University, Algeria, in 2005 and his Ph.D. in Mechanical Engineering from the National Polytechnic School, Algiers, in collaboration with the university of Western Switzerland from 2011, 2012 and 2013. He is the supervisor of many Ph.D. theses and masters in Algeria. Recently, he is reviewer in certain prestigious international journal. He has published more than 50 papers, and his research interests include the renewable energies, energy conversion and magnetocaloric materials.

Abdelhalim Tlemçani received the B.Sc. and M.Sc. degrees in power electronics and the Ph.D. degree in electrical engineering from the National Polytechnic School of Algiers, Algeria, in 1997, 1999 and 2007, respectively. In 2002, he was a lecturer and researcher with the Department of Electrical Engineering, Université Docteur Yahia Farès de Médéa, Médéa, Algeria, where he is currently a professor. He is the Director of the Control and Power Electronics Research Group. His research interests include power electronics, electrical drives, robust and nonlinear control, and fuzzy systems.

Arezki Smaili is a full professor of Mechanical Engineering and Director of Research Laboratory of Mechanical Engineering (Laboratoire de Génie Mécanique et Développement, LGMD), at Ecole Nationale Polytechnique (ENP), Algiers. He received his M.Sc. in Mechanical Engineering from Laval University, Québec (Canada), in 1991 and his Ph.D. in Energy Sciences from Université du Québec (Canada) in 1998. He joined the ENP in 2006. He was formerly research scientist in the Wind Energy Laboratory at Ecole de technologie supérieure, Montreal (Canada). He has been involved with wide range of energy conversion applications, particularly in the area of thermal analysis of renewable energy systems and aerodynamics of wind turbines since the 1992. He has supervised more than 10 Ph.D. theses, and his research has produced more than 100 technical papers published in international journals and proceedings.

Chapter 1
Fabrication of Flexible Photovoltaic Cells

Ourida Ourahmoun

Abstract Etching of Indium Tin Oxide (ITO) is an important step in the realization of organic photovoltaic cells. In the case of a glass substrate, the etching is carried out by hiding the areas that are to be preserved by varnish, then the samples are put in hydrochloric acid HCl, after that the samples will be cleaned in alcohols baths: acetone, ethanol and isopropanol. In the case of flexible substrates, the use of acetone to remove the varnish damages the plastic substrate. The solution to remedy this degradation is to use new technic which is photolithography. Flexible solar cells are made. The transparent electrode consists of ITO deposited on polyethylene terephthalate (PET). The active layer is composed on poly (3-hexylthiophene-2,5-diyl) (P3HT) and methyl ester of butyric acid [6,6]-phenyl C_{61} (PCBM). Poly (3,4-ethylenedioxythiophene)-polystyrene sulfonate of aluminum. The structure of the final device is: PET/ITO/PEDOT:PSS/P3HT:PCBM/Al. the results obtained show that photolithography etching is an efficient technic for determining the geometry of the electrodes without causing damage to the plastic substrates.

Keywords Photolithography · Flexible substrates · PET · Organic solar cells · Etching

1.1 Introduction

Organic solar cells have attracted much attention in the recent years due to their many intrinsic advantages: flexibility, low cost, solution processing, large quantities and easy device fabrication. Power conversion efficiency of 13% is achieved in devices with bilayer interlayer [1]. The reliability of organic solar cells is improved by using hybrid materials for electron transport [2]. A conversion efficiency of 8% is achieved using new small molecule donor [3]. Cells with electrodes without indium are produced, with a yield of about 3.5% [4]. Purely plastic cells are developed using PEDOT:PSS electrodes. The use of nanoparticles such as SiO_2 improves the

O. Ourahmoun (✉)
Electronic Department, University of Mouloud Mammeri of Tizi-Ouzou, 15000 Tizi Ouzou, Algeria

Y. Chiba et al. (eds.), *Advances in Green Energies and Materials Technology*,
Springer Proceedings in Energy, https://doi.org/10.1007/978-981-16-0378-5_1

performances of organic cells [5]. Replacing the hole transport layer PEDOT:PSS with the hydrophobic P3HT-Si improves the lifetime of the organic devices [6]. The electrical and optical properties of P3HT are very sensitive to the presence of oxygen and water, as well as in contact with the different metals and oxides that are used as electrodes [7]. It is necessary to encapsulate the cells to improve their stability and protect them against the causes of degradation. The conventional organic photovoltaic cell consists of a stack of five layers: the transparent anode (ITO), which is covered with a hole transport layer (HTL), the active layer, electron transport layer (ETL) and metallic cathode (Al). There are different TCOs used as electrodes, such as, ITO, ZnO, SnO_2, FTO Al-doped ZnO (AZO) and In-doped ZnO (IZO) [8]. To made purely flexible solar cells, conductive polymers are used such as graphene oxide (GO) and silver nanowire (AgNW) deposited on PET [9]. The flexible solar cells fabricated using the roll-to-roll technology exhibited a power conversion efficiency of 1.88% [10]. Multilayer structure anode structure enhances the performances of the cells [11]. The argon ion treatment of the polyethylene terephthalate (PET) substrate improve the flexibility of the ITO electrode [10]. The internal quantum efficiency of a solar cell depends on its intrinsic material properties, such as its crystallinity, energy band gap, carrier transport behavior and the number of defects and impurities [12]. Thermal annealing improves photocurrent as well as interface between organic layers and metal electrodes due to the reduction of interface defects [13]. Metallic nanogratings integrated with an indium tin oxide electrode is a possible approach to improve light absorption property in the active layer [14]. Several techniques are used to deposit the polymer layers onto flexible or glass substrates. Spin coating, doctor blading, printing, brush painting and roll-to-roll-technology [15]. Flexible tandem solar cells with polyether sulfone (PES) substrate showed the same efficiency with device on glass substrate [16]. The parameters of ITO such as resistivity, carrier concentration, transmittance, surface morphology and work function depend on the surface treatments and significantly influence the performances of the solar cells [17]. In this study the photolithography is used to define the electrode geometry of the flexible solar cells. A new Etching technology by photolithography for plastic substrate (PET/ITO) is presented. The parameters of the organic solar cells PET/ITO/P3HT:PCBM/Al and Glass/ITO/P3HT:PCBM/Al such as current density J(V), open circuit voltage V_{OC}, Fill Factor (FF), and the short current density (Jsc) are giving.

1.2 Fabrication Method of the Flexible Cell

1.2.1 ITO Etched by Photolithography

Polyethylene Terephthalate (PET) is used as substrate for flexible solar cells. The photolithographic process follows the following steps as shown in Fig. 1.1:

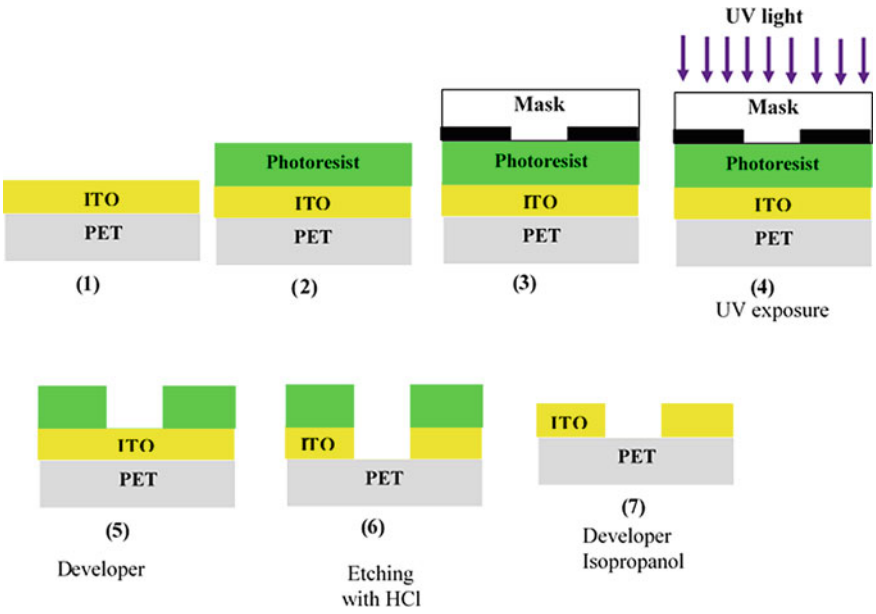

Fig. 1.1 Steps of photolithography process used to etch ITO

- The PET/ITO substrate is spin coated with a photoresist (resin S1828) to form uniform ~3 μm thin film on the surface.
- The substrate is exposed with ultraviolet light through a mask which contains a desired design of the electrodes. The photolithography device (Insolator) used to harden the resin is shown in Fig. 2A.

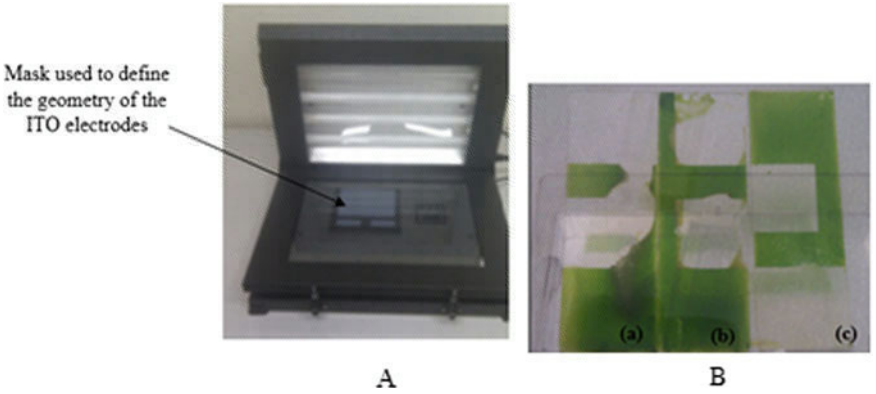

Fig. 1.2 **A** Insolator used to harden the photoresist S1828, **B** Influence of the emersion time of the resin PRP 200 in developer (sodium hydroxide) on the quality of the development; (a) t = 180 s, (b) t = 120 s and (c) t = 90 s

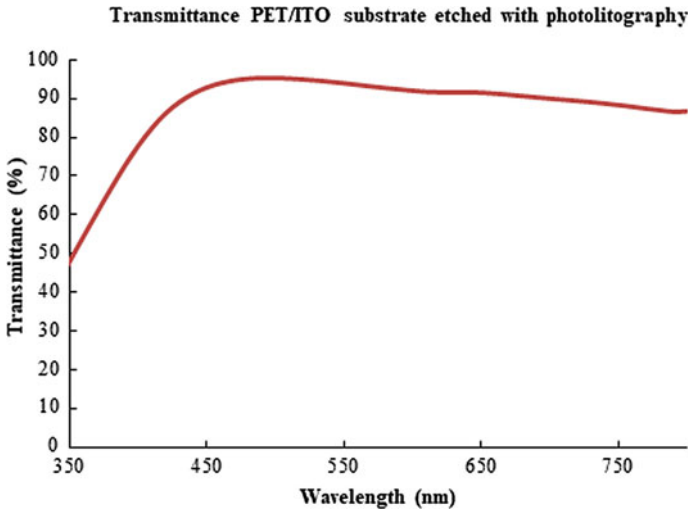

Fig. 1.3 Transmittance of the PET/ITO substrate after photolithography etching

- The photoresist is developed.
- The samples are etching with HCl heated at 90 °C.
- The samples were immersed in the developer to remove the photoresist. Finally, substrates were cleaned with isopropanol.

The advantages of this method is that acetone is not used. Because acetone damages the organic layers. For a concentration developer 1.5 g of sodium hydroxide in 200 ml of water, if the development time is greater than 90 s, there is overdevelopment as shown in Fig. 2B.a. The disadvantages of the resin PRP 200 is the presence of holes in ITO layer after etching, from which we opted for the use of the photosensitive resin S 1828 used in clean room. The optical properties of ITO etched using photolithography method are measured by means of UV transmittance device. The transmittance is taken about 90% in visible spectrum as shown in Fig. 1.3.

1.2.2 Realization of the Flexible Solar Cells

The flexible solar cell is based on a blend of poly(3-hexylthiophene-2,5-diyl) (P3HT) and [6,6]-phenyl C_{61} butyric acid methyl ester (PCBM). The PET substrate covered by transparent electrode indium tin oxide (ITO) are etched with photolithography technic, then treated by UV ozone for 30 min. Afterwards, polyethylene dioxythiophene:polystyrene sulfonate (PEDOT:PSS) was spin coated on the substrate in order to form a hole transport layer (HTL). A film about 180 nm thick of blend of P3HT:PCBM with a weight ratio of (1:1) in chlorobenzene was further spin coated on Pedot. Finally, an Al cathode (90 nm thick) was evaporated at 3.10^{-6} mbar, through

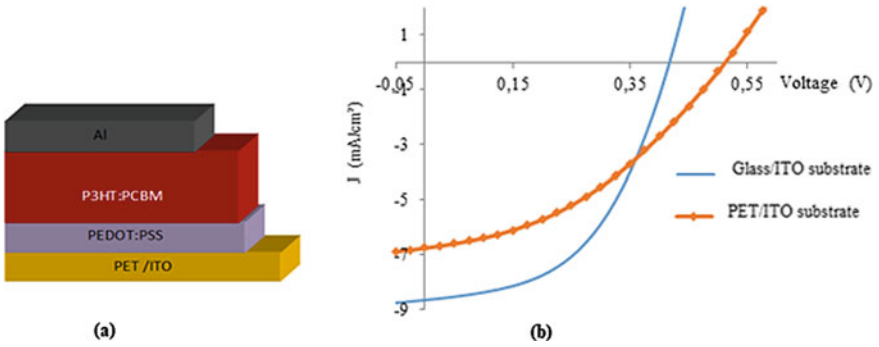

Fig. 1.4 a Structure of the organic solar cell with flexible substrate: PET/ITO/PEDOT:PSS/P3HT:PCBM/Al, **b** J-V characteristics under illumination of organic solar cells with Glass ITO substrate and PET/ITO substrate

a shadow mask delimiting à 0.18 cm^2 solar cell area. The cells are annealed at 110 °C for 30 min in the glove box. To compare between performances of organic solar cells with flexible substrate and cells with glass substrates, a structure with glass substrate is realized. The direct structure of the flexible solar cell realized is illustrated in Fig. 4a.

1.3 Results and Discussion

The J-V characteristics under standard AM1.5 illumination of the representative P3HT:PCBM cell with PET/ITO or Glass/ITO substrates were measured in the glove box. The light intensity of the solar simulator is 100 mW/cm^2. The results presented in Fig. 4b show that cells with glass substrates have better performances than with PET substrates. The difference in the performances is attributed to a decrease in current density (J_{SC}). J_{SC} of glass/ITO substrate is 8.87 mA/cm^2 and the J_{SC} of cells with PET/ITO is 6.67 mA/cm^2. The photocurrent generated is limited by transparency of the substrate, because the transparency of the glass substrate is slightly higher than the transparency of the flexible PET substrates. Even if the yield of flexible cells is lower than the yield of cells deposited on glass, flexible cells have several advantages. The advantage of using flexible substrates is the production of cheaper, lightweight, flexible photovoltaic cells with larges areas and unbreakable.

1.4 Conclusion

The use of acetone to remove the varnish and the cleaning of plastic substrates is unhelpful as the acetone damages the organic layers. The solution found for etching

the ITO deposited on PET without using acetone is photolithography. This method is non-destructive and gives interesting results. Results show that photolithography is an efficient technic for the realization of flexible organic solar cells. to improve the performance of flexible photovoltaic cells it is necessary to optimize the etching parameters of the ITO, such as: the thickness of the photoresist, the duration of the development, the concentration of the developer, the thermal annealing, the duration of exposure to the UV radiation of the insolator.

Photovoltaic devices including dye solar cells, organic solar cells and perovskite solar cells can be made flexible using plastic substrates (PET or PEN), so it is necessary to understand and master the manufacturing technology including the etching of substrates.

References

1. M.B. Upama, N.K. Elumalai, M.A. Mahmud, C. Xu, D. Wang, M. Wright, A. Uddin, Enhanced electron transport enables over 12% efficiency by interface engineering of non-fullerene organic solar cells. Solar Energy Mater. Sol. Cells **187**, 273–282 (2018)
2. Z. Li, Z.C. Liu, J. Guo, Y. Zhou, I. Shen, W. Guo, Passivation effect of composite organic interlayer on polymer solar cells. Org. Electron. **63**, 129–136 (2018)
3. C. Ye, Y. Wang, Z. Bi, X. Guo, Q. Fan, J. Chen, M. Zhang, High-performance organic solar cells based on a small molecule with thieno [3, 2-b] thiophene as π-bridge. Org. Electron. **53**, 273–279 (2018)
4. U.J. Lee, S.H. Lee, J.J. Yoon, S.J. Oh, S.H. Lee, J.K. Lee, Surface interpenetration between conducting polymer and PET substrate for mechanically reinforced ITO-free flexible organic solar cells. Sol. Energy Mater. Sol. Cells **108**, 50–56 (2013)
5. P. Shao, X. Chen, X. Guo, W. Zhang, F. Chang, Q. Liu, D. He, Facile embedding of SiO_2 nanoparticles in organic solar cells for performance improvement. Org. Electron. **50**, 77–81 (2017)
6. H. Awada, G. Mattana, A. Tournebize, L. Rodriguez, D. Flahaut, L. Vellutini, S. Chambon, Surface engineering of ITO electrode with a functional polymer for PEDOT: PSS-free organic solar cells. Org. Electron. **57**, 186–193 (2018)
7. G.C. Faria, D.J. Coutinho, H. Von Seggern, R.M. Faria, Doping mechanism in organic devices: effects of oxygen molecules in poly (3-hexylthiophene) thin films. Org. Electron. **57**, 298–304 (2018)
8. M. Murugesan, D. Arjunraj, J. Mayandi, V. Venkatachalapathy, J.M. Pearce, Properties of Al-doped zinc oxide and In-doped zinc oxide bilayer transparent conducting oxides for solar cell applications. Mater. Lett. **222**, 50–53 (2018)
9. K. Naito, R. Inuzuka, N. Yoshinaga, W. Mei, Transparent conducting films composed of graphene oxide/Ag nanowire/graphene oxide/PET. Synth. Met. **237**, 50–55 (2018)
10. K.H. Choi, J.A. Jeong, J.W. Kang, D.G. Kim, J.K. Kim, S.I. Na, H.K. Kim, Characteristics of flexible indium tin oxide electrode grown by continuous roll-to-roll sputtering process for flexible organic solar cells. Sol. Energy Mater. Sol. Cells **93**(8), 1248–1255 (2009)
11. H.W. Tsai, Z. Pei, C. Chen, S.J. Cheng, W.S. Hsieh, P.W. Li, Y.J. Chan, Anode engineering for photocurrent enhancement in a polymer solar cell and applied on plastic substrate. Sol. Energy Mater. Sol. Cells **95**(2), 611–617 (2011)
12. S.Y. Chuang, C.C. Yu, H.L. Chen, W.F. Su, C.W. Chen, Exploiting optical anisotropy to increase the external quantum efficiency of flexible P3HT: PCBM blend solar cells at large incident angles. Sol. Energy Mater. Sol. Cells **95**(8), 2141–2150 (2011)

13. S. Kim, S. Ryu, Efficiency of flexible organic solar cells as a function of post-annealing temperatures. Curr. Appl. Phys. **10**(4), 181–184 (2010)
14. D.A. Gollmer, F. Walter, C. Lorch, J. Novák, R. Banerjee, J. Dieterle, M. Fleischer, Fabrication and characterization of combined metallic nanogratings and ITO electrodes for organic photovoltaic cells. Microelectron. Eng. **119**, 122–126 (2014)
15. S.W. Heo, K.W. Song, M.H. Choi, T.H. Sung, D.K. Moon, Patternable solution process for fabrication of flexible polymer solar cells using PDMS. Sol. Energy Mater. Sol. Cells **95**(12), 3564–3572 (2011)
16. B.J. Lee, H.J. Kim, W.L. Jeong, J.J. Kim, A transparent conducting oxide as an efficient middle electrode for flexible organic tandem solar cells. Sol. Energy Mater. Sol. Cells **94**(3), 542–546 (2010)
17. Y.T. Cheng, J.J. Ho, C.K. Wang, W.L. Lee, C.C. Lu, B.S. Yau, K.L. Wang, Improvement of organic solar cells by flexible substrate and ITO surface treatments. Appl. Surf. Sci. **256**(24), 7606–7611 (2010)

Chapter 2
Effect of Solution Concentration in the Optical and Electrical Properties of Copper Oxide Thin Films

L. Herissi, L. Hadjeris, Z. Moussa, L. Hafsa, S. Djebabra, B. Herissi, A. Sari, and S. Bouchrit

Abstract The aim of this work is the study of the effect of solution concentration in the optical and electrical properties of copper oxide thin films deposited by ultrasonic spray pyrolysis technique in order to obtain good photoelectric properties which makes it an important candidate in many technological applications. These films are elaborated onto glass substrates from an aqueous solution of copper (II) chloride dihydrate with different solution concentrations. Substrate temperature, nozzle-substrate distance, and deposition time were kept constant during the whole deposition process. After the deposition, we annealed these films in air at 400 °C for 120 min. UV-Visible spectrophotometry and the four-point method were used to evaluate the optical and electrical properties, the films obtained are p-type semiconductors, high optical absorption in the UV-Visible domains, rough surface with good adhesion to the substrate. Optical and electrical properties of undoped copper oxide thin films varied by the variation of solution concentration.

Keywords Thin films · Copper oxide · Spray pyrolysis · Annealing · Solution concentration · Electrical properties · Optical absorption

2.1 Introduction

Copper forms two different oxides such as cupric oxide (CuO) and cuprous oxide (Cu_2O). CuO is a black color material, n-type semiconductor with bandgap of 1.21–1.51 eV [1, 2]. Cu_2O is a brown yellowish material, p-type semiconductor and has a bandgap of 2.1 eV [1]. Spray pyrolysis deposition (SPD) has the advantages of set-up easiness, cost-effective, and flexibility over the plasma film deposition methods

L. Herissi (✉) · A. Sari · S. Bouchrit
Matter Sciences Department, Larbi Tebessi University, 12000 Tebessa, Algeria

L. Herissi · L. Hadjeris · Z. Moussa · L. Hafsa · S. Djebabra
LMSSEF, Larbi Ben M'Hidi University, 04000 Oum El Bouaghi, Algeria

B. Herissi
Department of Electronic and Telecommunication, University 8 May 1945, 24000 Guelma, Algeria

Y. Chiba et al. (eds.), *Advances in Green Energies and Materials Technology*,
Springer Proceedings in Energy, https://doi.org/10.1007/978-981-16-0378-5_2

[3]. Large surface CuO films can thus be deposited under atmospheric conditions on substrates from low-priced chemicals, while monitoring the preparation process step by step [4]. However, the physical and chemical properties of the films thus prepared depend on the process parameters [5]. The aim of this work is to study the experimental conditions in order to obtain optimum deposition parameters yielding CuO films with the desired physical properties for particular applications.

2.2 Experimental Procedure

The copper oxide films were deposited by ultrasonic spray pyrolysis technique (Fig. 2.1) from solution of copper (II) chloride dihydrate ($CuCl_2{\cdot}2H_2O$) dissolved in doubly distilled water onto glass substrates with different solution concentration (0.02, 0.04, 0.05, 0.08, and 0.1 mol/l). Substrate temperature, nozzle-substrate distance, and deposition time were kept constant during the whole deposition process at 300 °C, 3 cm, and 5 min, respectively. After the deposition, we annealed these films in air at 400 °C for 120 min.

The transmittance of the films deposited on glass was measured in the UV-Visible region using a double beam spectrophotometer (Shimadzu 3101PC). The gap energy E_g of the ZnO films deposited on glass substrates was determined from their transmittance T (λ). The absorption coefficient α (λ), in the spectral region of absorption of the light, was deduced from the Beer-Lambert law [6]:

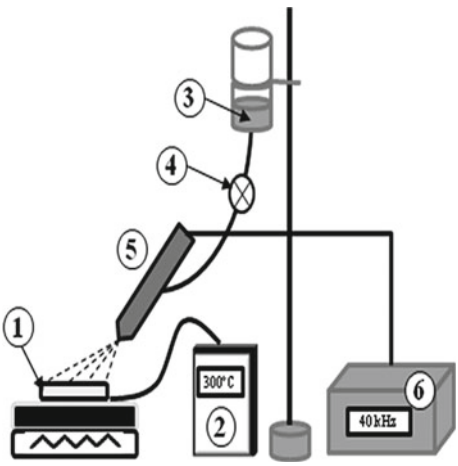

Fig. 2.1 Experimental device used to deposit thin films by ultrasonic spray pyrolysis technique; **1**. Glass substrates on an electrical resistance, **2**. Digital thermocouple, **3**. Solution to deposit, **4**. Flow rate controller, **5**. Nozzle, and **6**. Ultrasonic generator

$$\alpha = \frac{1}{d} \ln\left(\frac{100}{T(\%)}\right) \tag{2.1}$$

That according to the Tauc's theory for the direct allowed transitions such as those occurring in the direct gap of CuO, α (hν) close to the band edge is [3]:

$$(\alpha h\upsilon)^n = A(h\upsilon - E_g) \tag{2.2}$$

where A is a constant of proportionality and hν is the energy of the incidental light photons. Eg can be estimated by extrapolating to the hν—axis the linear part of the $(\alpha h\nu)^2$ curve.

The film thickness and refractive index were deduced from the Swanepoel's envelope method that are deduced from the variation of the optical transmittance as a function of the wavelength for each film which gives very convergent values [7]. The typical variation of (Lnα) versus photon energy of copper oxide thin film for deduce the Urbach energy, which is related to the disorder in the film network, is expressed as [8]:

$$\alpha = \alpha_0 . \exp\left(\frac{h\upsilon}{E_{00}}\right) \tag{2.3}$$

Electrical conductivity were measured using four-point-probe method by the following expression [8]:

$$\sigma = \frac{\ln 2}{\pi . d} . \frac{I}{V} \tag{2.4}$$

2.3 Results and Discussions

Figure 2.2 shows the typical spectra of the variation of the optical transmittance of copper oxide thin films as a function of the wavelength of incident photon in the UV-Vis-NIR range (200–1100 nm) obtained from the solution of copper (II) chloride dihydrate prepared by ultrasonic spray pyrolysis technique with precise experimental conditions after annealing under air for $t_R = 120$ min at $T_R = 400$ °C.

In this work, the values of the optical transmittance at 1100 nm are decreased before annealing from 53 to 22% and 51 to 16% after annealing with the increase of the solution concentration from 0.02 to 0.08 mol/l. The decrease in optical transmittance by increasing the solution concentration may be due to the increase in the thickness of the thin films and its surface roughness [9], and also the color change of our films [2]. The optical transmittance of the sample of 0.1 mol/l and more transparent compared to the sample of 0.08 mol/l since the film made with a high molarity (0.1 mol/l) is more porous than the sample of 0.08 mol/l [10]. As can also be note that

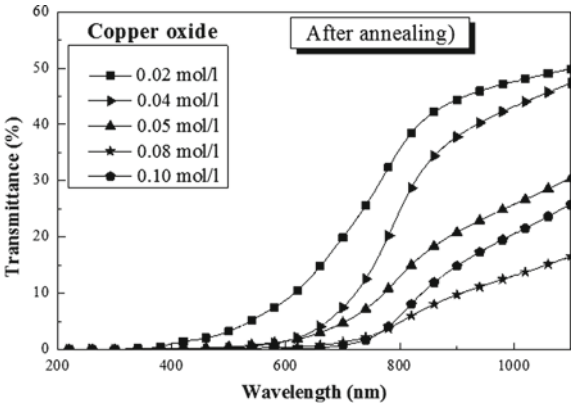

Fig. 2.2 Variation of optical transmittance of copper oxide thin films versus wavelength for different values of the solution concentration after annealing under air

the increase of the solution concentration leads to a displacement of the absorption threshold towards the long wavelengths. By annealing, the optical transmittance at $\lambda = 1100$ nm of all films is decreased slightly by comparing with the spectrum of the optical transmittance before annealing, this decrease can be explained by the decrease of the porosity, the surface roughness and the vacuum in the layers "$T(\lambda < 300\ \text{nm}) = 0\%$" by annealing. It is also observed that the annealing decrease difference (δT) is decreased with the increase in energy of the incident photons.

Figure 2.3 shows the variation of the film thickness and refractive index of copper oxide (Cu_xO) after annealing under air as a function of the solution concentration.

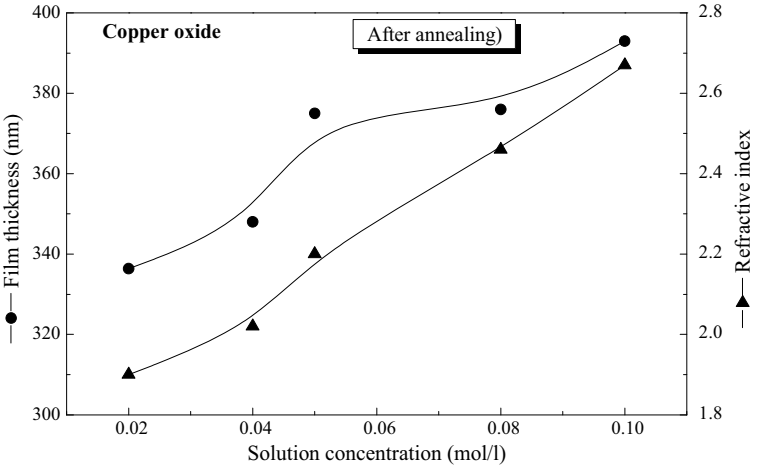

Fig. 2.3 Variation of the film thickness and refractive index of copper oxide thin films versus wavelength for different values of the solution concentration after annealing under air

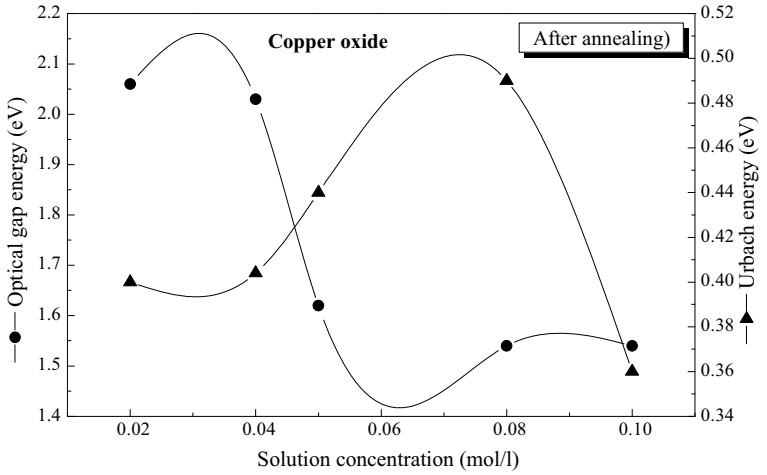

Fig. 2.4 Variation of the optical gap energy and Urbach energy of copper oxide thin films versus wavelength for different values of the solution concentration after annealing under air

With the increase the concentration of solution from 0.02 to 0.1 mol/l, the both increase of the film thickness and refractive index of copper oxide (Cu_xO) from 336 to 393 nm and 1.9 to 2.7, respectively. As can be interpreted these increases by the increase in the quantity of material deposited (there is more material which contributes to the formation of the film), the existence of the porosity in the film, the gradation in color (light brown to black) with the increase in the concentration of solution [9, 11].

Figure 2.4 shows the variation of the optical gap energy and Urbach energy of copper oxide (Cu_xO) after annealing under air as a function of the solution concentration. With the increase the concentration of solution from 0.02 to 0.1 mol/l, the E_g decreasing is due to the increase in both the Urbach energy and the refractive index, several authors have found an indirect correlation between the Urbach energy and the optical gap energy [11]. This remark can be explained by the decrease of the grain size, more disorder, the gradation in color (light brown to black) with the increase in the solution concentration [9–11].

The E_g is decrease with the increase of the concentration of solution, it is noted that the optical gap values indicate that the films deposited at 0.02 and 0.04 mol/l have cuprous oxide (Cu_2O) phase structures, whereas the films deposited at 0.05 and 0.08, and 0.1 mol/l have cupric oxide (CuO) phase structures [2]. This phase difference is due to the kinetics of the formation of copper oxides during thin film deposition which depends on a number of factors such as the solution concentration and the amount of deposited materials [11]. The minimum value of the Urbach energy of the film deposited at 0.1 mol/l is logical, reason why this sample has a single crystalline phase and its optical gap is closer to the solid state of CuO [12]. Figure 2.5 shows the influence of the solution concentration on the electrical conductivity of thin films.

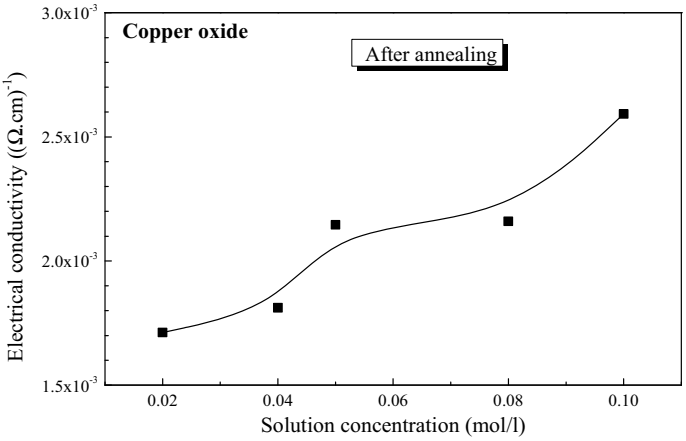

Fig. 2.5 Variation of the electrical conductivity of copper oxide thin films as a function of solution concentration

The electrical conductivity of the films increases with the increase of the concentration of solution. These increases can be interpreted by increasing the concentration of charge carriers [10, 11], and also the effect of phase change in the sample structure (from Cu_2O to CuO) [2].

2.4 Conclusion

Copper oxide thin films deposited onto glass substrates by ultrasonic spray pyrolysis technique with different solution concentrations. The films obtained are p-type semiconductors, high optical absorption in the UV-Visible domains, rough surface with good adhesion to the substrate. Optical and electrical properties of copper oxide thin films varied by the variation of solution concentration.

References

1. R.P. Wijesundera, M. Hidaka, K. Koga, J.Y. Choi, N.E. Sung, Structural and electronic properties of electrodeposited heterojunction of CuO/Cu_2O. Ceramics-Silikàty **54**, 19–25 (2010)
2. A.H. Jayatissa, K.A. Guo, C. Jayasuriya, Fabrication of cuprous and cupric oxide thin films by heat treatment. Appl. Surface Sci. **255**, 9474–9479 (2009)
3. L. Herissi, L. Hadjeris, M.S. Aida, J. Bougdira, Properties of $(NiO)_{1-x}(ZnO)_x$ thin films deposited by spray pyrolysis. Thin Solid Films **605**, 116–120 (2016)
4. S. Roy, S. Basu, Improved zinc oxide film for gas sensor applications. Bull. Mater. Sci. **25**, 513–515 (2002)

5. W.T. Seeber, M.O. Abou-Helala, S. Bartha, D. Beila, T. HoÈ chea, H.H. Afify, S.E. Demian, Transparent semiconducting ZnO:Al thin films prepared by spray pyrolysis. Mater. Sci. Semicond. Process. **2**, 45–55 (1999)
6. A. Bougrine, A. El Hichou, M. Addou, J. Ebothé, A. Kachouna, M. Troyon, Structural, optical and cathodoluminescence characteristics of undoped and tin-doped ZnO thin films prepared by spray pyrolysis. Mater. Chem. Phys. **80**, 438–445 (2003)
7. L. Herissi, L. Hadjeris, M.S. Aida, S. Azizi, A. Hafdallah, A. Ferdi, Ni-doped ZnO thin films deposited by pneumatic spray pyrolysis. Nano Hybrids Compos. **27**, 21–29 (2019)
8. L. Mustafa, S. Anjum, S. Waseem, S. Bashir, K. Mahmood, M. Saleem, E. Ahmad, Structural and optical properties of ZnO co-doped with Co and Ni thin films deposited by pulse laser deposition technique. Optik **161**, 54–63 (2018)
9. F.Z. Chafi, A. Hadri, C. Nassiri, B. Fares, L. Laanab, N. Hassanain, A. Mzerd, Undoped CuO deposited by spray pyrolysis technique. J. Mater. Environ. Sci. **7**, 170–175 (2016)
10. L. Herissi, L. Hadjeris, H. Moualkia, N. Abdelmalek, N. Attaf, M.S. Aida, J. Bougdira, Realization and study of ZnO thin films intended for optoelectronic applications. J. New Technol. Mater. **1**, 39–43 (2011)
11. L. Herissi, L. Hadjeris, N. Attaf, M.S. Aida, A. Hafdallah, W. Daranfad, Réalisation et étude de couches minces de ZnO transparentes et conductrices. Alger. J. Adv. Mater. **4**, 415–418 (2008)
12. A. Jareeze, Optical properties, structure, and morphology of CuO grown by thermal oxidation of Cu thin film on glass substrate. J. Kufa Phys. **6**, 36–41 (2014)

Chapter 3
IR Spectroscopy and Computational Study of Structural, Vibrational and Electronic Properties of Hydrindantin Dihydrate

Abdelali Boukaoud, Younes Chiba, Khoukha Fatimi, Nassima Yahimi, Fatima Zohra Meguellati, and Souad Bouguettaya

Abstract The experimental FT-IR spectrum of hydrindantin dihydrate ($C_{18}H_{10}O_6.2H_2O$) has been investigated for the first time. The vibrational spectral signatures of OH stretching modes have been analyzed by using the results of density functional theory (DFT) calculations performed in the solid state. These results have shown that the IR bands due to the asymmetric ($\upsilon_{as}OH$) and symmetric ($\upsilon_{s}OH$) stretching modes of water molecules are overlapped in the large band centered at 3433 cm^{-1} in the experimental spectrum. While, the stretching bands due to the OH groups of hydrindantin molecules are red shifted to 2831 cm^{-1} owing to the formation of strong inter-molecular O–H···O hydrogen bonds with adjacent water molecules. Moreover, this study has been extended to reveal some calculated electronic properties of the isolated hydrindantin molecule.

Keywords Hydrindantin dihydrate · IR spectroscopy · DFT calculations · H-bonds

A. Boukaoud (✉)
Laboratoire de Physique des Techniques Expérimentales et ses Applications, Université de Médéa, Medea, Algeria
e-mail: boukaoud.abdelali@univ-medea.dz

Y. Chiba
Department of Mechanical Engineering, Faculty of Science and Technology, University of Medea, Medea, Algeria

A. Boukaoud · K. Fatimi · N. Yahimi · F. Z. Meguellati · S. Bouguettaya
Département des Sciences de la Matière, Faculté des Sciences, Université de Médéa, Medea, Algeria

Y. Chiba et al. (eds.), *Advances in Green Energies and Materials Technology*,
Springer Proceedings in Energy, https://doi.org/10.1007/978-981-16-0378-5_3

3.1 Introduction

Hydrindantin dihydrate ($C_{18}H_{10}O_6$. $2H_2O$) can be used as a reagent for the determination of amino acids [1]. In the solid state, the hydrindantin and water molecules are linked by inter-molecular O–H···O hydrogen bonds (H-bonds) to form a three dimensional molecular arrangement. These interacting molecules are also linked by inversion centers which coincide with the symmetry centers of hydrindantin molecules [2].

The incorporation of H_2O molecules into the crystal structure of the under-investigated compound will certainly complicate the assignment of the observed IR bands in the OH stretching region. In some cases, the knowledge of crystallographic information, especially the H-bond geometries, can to some extent facilitate the assignment of the IR bands arising from the OH stretching vibrations [3]. However, the best way to assign such bands is to compare the results of DFT performed in the solid state with the experimental ones obtained from the vibrational spectra [4]. Here, a combination of theoretical and experimental studies is performed to explore the OH stretching region of the experimental IR spectrum of the titled compound.

To the best of our knowledge, the current study is the first which analyses the vibrational behavior and electronic properties of hydrindantin dihydrate using IR spectroscopy and DFT calculations. Thus, we hope here to achieve two main aims: the first one is to better understand the H-bonding effects on the vibrational modes in order to properly assign the measured IR bands situated in the region 1400–3400 cm^{-1}. The second aim is devoted to study theoretically some electronic properties of the isolated hydrindantin molecule.

3.2 Experimental Details

A commercial sample of hydrindantin dihydrate, in powder form, was used without further purification to prepare a mixture containing 1% of hydrindantin dihydrate and 99% of potassium bromide (KBr). The mixture was then pressed to form a pellet for the IR spectral measurements. The obtained spectrum was recorded at room temperature in the wavenumber range of 400–4000 cm^{-1}, using a FTIR-8400 Spectrometer. The spectral resolution of the spectrometer was 4 cm^{-1}.

3.3 Computational Details

All the periodic DFT calculations presented here were carried out by using the GGA (generalized gradient approximation) at the PBE (Perdew–Burke–Ernzerhof) functional [5]. The norm-conserving pseudopoentials were used to describe the ion-electron interactions and a kinetic energy cutoff of 830 eV of the plane-wave basis

set was used. The harmonic vibrational wavenumbers are calculated at the Γ point employing the DFPT (density functional perturbation theory) [6].

On the other hand, all the non-periodic DFT calculations were preformed in the gas phase using the B3LYP functional [7, 8] and the 6-311G(d,p) basis set.

3.4 Results and Discussion

3.4.1 Structural Optimization

Figure 3.1a shows the optimized molecular structure of hydrindantin in the gas phase obtained by the B3LYP functional. The optimized crystal structure of hydrindantin-$2H_2O$ in the solid phase is presented in Fig. 3.1b.

In agreement with the experimental results [2], our calculations show that hydrindantin-$2H_2O$ adopts the monoclinic system with the space group $P2_1/c$. The calculated lattice parameters in comparison with the experimental ones are listed in Table 3.1.

The H-bonds present in hydrindantin-$2H_2O$ crystal are clearly shown in Fig. 3.1b. In accordance with the previously reported crystal structure [2], each molecule, hydrindantin/water, is hydrogen donor in two inter-molecular O–H···O H-bonds. Table 3.2 shows a comparison between the calculated H-bond geometries and the corresponding ones obtained from the X-Ray experiment.

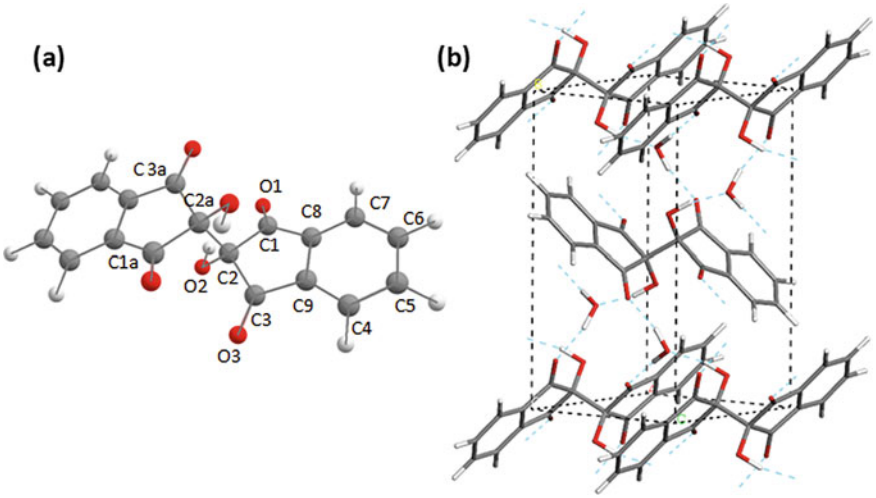

Fig. 3.1 Optimized structures obtained by DFT calculations: **a** optimized molecular structure of hydrindantin in the gas phase; **b** optimized unit cell of hydrindantin-$2H_2O$ in the solid phase